Ice core age dating and paleothermometer calibration based on isotope and temperature profiles from deep boreholes at Vostok Station (East Antarctica)

Andrey Salamatin, Vladimir Lipenkov, Nartsiss Barkov, Jean Jouzel, Jean Robert Petit, Dominique Raynaud

▶ **To cite this version:**

Andrey Salamatin, Vladimir Lipenkov, Nartsiss Barkov, Jean Jouzel, Jean Robert Petit, et al.. Ice core age dating and paleothermometer calibration based on isotope and temperature profiles from deep boreholes at Vostok Station (East Antarctica). Journal of Geophysical Research: Atmospheres, 1998, 103 (D8), pp.8963-8977. 10.1029/97JD02253 . hal-03110403

HAL Id: hal-03110403
https://hal.science/hal-03110403

Submitted on 14 Jan 2021

HAL is a multi-disciplinary open access archive for the deposit and dissemination of scientific research documents, whether they are published or not. The documents may come from teaching and research institutions in France or abroad, or from public or private research centers.

L'archive ouverte pluridisciplinaire **HAL**, est destinée au dépôt et à la diffusion de documents scientifiques de niveau recherche, publiés ou non, émanant des établissements d'enseignement et de recherche français ou étrangers, des laboratoires publics ou privés.

JOURNAL OF GEOPHYSICAL RESEARCH, VOL. 103, NO. D8, PAGES 8963–8977, APRIL 27, 1998

Ice core age dating and paleothermometer calibration based on isotope and temperature profiles from deep boreholes at Vostok Station (East Antarctica)

Andrey N. Salamatin,[1] Vladimir Y. Lipenkov,[2] Nartsiss I. Barkov,[2] Jean Jouzel,[3] Jean Robert Petit,[4] and Dominique Raynaud[4]

Abstract. An interpretation of the deuterium profile measured along the Vostok (East Antarctica) ice core down to 2755 m has been attempted on the basis of the borehole temperature analysis. An inverse problem is solved to infer a local "geophysical metronome," the orbital signal in the surface temperature oscillations expressed as a sum of harmonics of Milankovich periods. By correlating the smoothed isotopic temperature record to the metronome, a chronostratigraphy of the Vostok ice core is derived with an accuracy of ±3.0–4.5 kyr. The developed timescale predicts an age of 241 kyr at a depth of 2760 m. The ratio $\delta D/\delta T_i$ between deuterium content and cloud temperature fluctuations (at the top of the inversion layer) is examined by fitting simulated and measured borehole temperature profiles. The conventional estimate of the deuterium-temperature slope corresponding to the present-day spatial ratio (9 per mil/°C) is confirmed in general. However, the mismatch between modeled and measured borehole temperatures decreases noticeably if we allow surface temperature, responsible for the thermal state of the ice sheet, to undergo more intensive precession oscillations than those of the inversion temperature traced by isotope record. With this assumption, we obtain the long-term temporal deuterium-temperature slope to be 5.8–6.5 per mil/°C which implies that the glacial-interglacial temperature increase over central Antarctica was about 15°C in the surface temperature and 10°C in the inversion temperature. Past variations of the accumulation rate and the corresponding changes in the ice-sheet surface elevation are simultaneously simulated.

1. Introduction

It is well recognized that ice cores from deep boreholes in Greenland and Antarctica, particularly at Vostok Station (East Antarctica), contain various palaeoclimatic signals of high resolution [e.g., *Lorius et al.*, 1985; *Barnola et al.*, 1987; *Genthon et al.*, 1987; *Jouzel et al.*, 1987, 1993, 1996; *Petit et al.*, 1990; *Chappellaz et al.*, 1990; *Sowers et al.*, 1993; *Dansgaard et al.*, 1993]. The two principal problems that arise in the ice core data interpretation and on which we focus further are (1) ice core age dating and (2) converting the measured isotope records into past temperature changes. The chronology is traditionally obtained by direct modeling of ice sheet dynamics and by computation of ice-flow lines [*Lorius et al.*, 1985; *Ritz*, 1992; *Jouzel et al.*, 1993; *Dansgaard et al.*, 1993], while isotope-to-temperature conversion is based on the contemporary spatial slopes of isotope-surface temperature linear relationships which were empirically established for Antarctica [*Lorius and Merlivat*, 1977; *Dahe et al.*, 1994] and Greenland [*Dansgaard et al.*, 1973; *Johnsen et al.*, 1989] and reproduced by Rayleigh-type modeling [*Dansgaard*, 1964; *Jouzel and Merlivat*, 1984]. These approaches, being fundamentally fruitful, are not devoid of difficulties and drawbacks in their practical implementations.

The uncertainty of the extended glaciological timescale (EGT) suggested for Vostok ice cores reaches, for instance, ±20 kyr at a depth of 2500 m [*Jouzel et al.*, 1993] mainly due to lack of knowledge about the current accumulation rate upstream of Vostok [*Ritz*, 1992]. EGT has recently been corrected (linearly compressed in time) within its deeper part to match the sequence of marine stages discovered in the ice core palaeoclimatic records from the depths 2546–2755 m [*Jouzel et al.*, 1996]. The estimated accuracy of the refined timescale is ±6 kyr. Another way of ice dating is to develop a common temporal framework on the basis of SPECMAP chronology [*Martinson et al.*, 1987] by correlating ice-core climate records with corresponding time series from ocean sediments [e.g., *Petit et al.*, 1990; *Pichon et al.*, 1992; *Shackleton et al.*, 1992; *Sowers et al.*, 1993; *Waelbroeck et al.*, 1995]. The latter is an important step toward a comparison of glaciological and oceanic palaeoclimate archives, although, in this case, besides the inherited errors of the tuning procedures, ±2.5–3.5 kyr [*Martinson et al.*, 1987], we fall into uncertainties which arise from comparing signals of different origins. Additional errors may also be encountered if the age of the air bubbles trapped in polar ice is involved [*Barnola et al.*, 1991; *Sowers et al.*, 1992, 1993], because of the ice age-gas age difference. The total accuracy is expected to be not better than ±5–6 kyr. Direct tuning of the Vostok deuterium record to insolation "metro-

[1]Department of Applied Mathematics, Kazan State University, Kazan, Russia.
[2]Arctic and Antarctic Research Institute, St. Petersburg, Russia.
[3]Laboratoire de Modélisation du Climat et de l'Environnement, Gif-sur-Yvette, France.
[4]Laboratoire de Glaciologie et Géophysique de l'Environnement, St.-Martin-d'Hères, France.

Copyright 1998 by the American Geophysical Union.

Paper number 97JD02253.
0148-0227/98/97JD-02253$09.00

nomes," recently attempted by *Waelbroeck et al.* [1995], seems to be more efficient since it avoids some of the above mentioned uncertainties. Nevertheless, the error in determining phase shifts between insolation and the Vostok record leads to an overall error of at least ±4 kyr in the dating. This is thought to be at the accuracy limit of tuning approaches because of the nonlinear climatic response to orbital forcing (climatic noise), estimated as ±4 kyr by *Imbrie et al.* [1992].

As far as conversion of isotope record into palaeotemperature record is concerned, the main uncertainties are due to the assumption that the local temporal and contemporary spatial isotope-temperature relationships are identical [*Dansgaard et al.*, 1973; *Lorius et al.*, 1985]. The recent study by *Jouzel et al.* [1994] based on the GCM analysis shows that for East Antarctica the corresponding relative error may be of the order of 30%. It should also be emphasized that ice core isotope records directly represent only climatic variations of the mean temperature in clouds where precipitation forms, i.e., the temperature T_i at the top of the inversion layer. T_i differs from the temperature T_s in the upper layer of snow-firn deposits where the boundary conditions are imposed on the thermal state of an ice sheet [*Robin*, 1977]. In addition, the response of T_i and T_s to the orbitally induced perturbations may also not be identical due to the complex nonlinear heat balance at the glacier surface, including thermal radiation and heat exchange with the atmosphere. For instance, higher precession oscillations of seasonal temperatures in comparison with the annual temperature variations predicted for central Antarctica by *Short et al.* [1991] could considerably influence the inversion strength $T_i - T_s$, which reaches its maximum in winter. We would stress that hereinafter, T_s is not only distinguished from T_i but is also not supposed to be equal to the near-surface air temperature. Consequently, the variations of the ice sheet surface temperature (δT_s) might be not merely proportional to those of the inversion temperature (δT_i), as it was suggested by *Jouzel et al.* [1987], and present-day borehole temperature profile may not be just a plain memory of the scaled ice core isotope record ($\delta\,^{18}O$ or δD), as it was assumed by *Ritz* [1989].

An advance in the interpretation of ice core data could be achieved by taking into account related information from other sources. From this point of view borehole-temperature profiles (especially in the central regions of large and thick ice sheets) could provide another unique piece of relevant information [*Robin*, 1976; *Budd and Young*, 1983; *Dahl-Jensen and Johnsen*, 1986; *Ritz*, 1989; *Palaeogeography, Palaeoclimatology, Palaeoecology*, 1992]. Certainly, the value of paleosignals remembered in borehole temperature profiles is limited because of their low resolution and comparatively "short memory." These signals are damped by heat diffusion process and do not contain high-frequency details as well as far-past history of surface temperature fluctuations. However, the main climatic cycles and corresponding major events (peaks and troughs in surface temperature variations) could be restored and their ages predicted if we assume them to be orbitally driven. Such an approach to isotope record dating has recently been developed and employed to deduce the chronology of the 2083-m-long Vostok ice core [*Salamatin et al.*, 1994, 1995]. The method is based on correlation of the isotopic temperature record to the local climatic "metronome," inferred from the borehole temperature measurements. It effectively incorporates the information about past temperature variations remembered in the ice thickness: time-averaged constant phase differences between oscillations of Earth's orbital elements and corresponding Milankovich cycles dominating in palaeotemperature response [*Imbrie et al.*, 1992, 1993] are automatically taken into account. Although this procedure does not eliminate the basic errors of tuning approaches, it presents an alternative way for ice-core dating. On the other hand, the studies by *Budd and Young* [1983], *Cuffey et al.* [1994, 1995], and *Johnsen et al.* [1995] convincingly show the usefulness of borehole temperature for calibrating the isotopic palaeothermometer.

In this paper we match the stacked 2755-m ice core deuterium record [*Jouzel et al.*, 1996] and high-precision temperature profile [*Salamatin et al.*, 1994] obtained from the deep boreholes drilled at Vostok Station. First, in section 2 we describe generally a mathematical model which relates inversion temperature variations (δT_i) to accumulation-rate and surface elevation changes and predicts the present-day temperature distribution in the ice sheet thickness in accordance with the past temperature fluctuations (δT_s) on the glacier surface. Then, in section 3 an inverse problem is formulated and solved to deduce the dominant (orbitally driven) metronomic part of the local palaeotemperature oscillations from the borehole temperature distribution. The correlation of the main climatic events (peaks and troughs) resolved in the "geophysical metronome" to those in the ice-core isotope record is performed in section 4. The latter procedure results in the Vostok age-depth relation. In section 5 the borehole temperature profile is used to calibrate the isotopic palaeothermometer and to reconstruct past temperature variations on the basis of the stacked deuterium record. Some other glaciological implications are also discussed in section 6.

2. General Parametric Description of the Model

First, when inferring past temperature variations on the ice sheet surface and, second, when adjusting the isotope-temperature relationship according to a borehole temperature profile, we need a mathematical model as well as a corresponding computational procedure which would couple the climatic input with the inner heat-and-mass-transfer processes in the glacier body, particularly, with the evolution of its temperature field T in time t.

The model we use here has been sequentially elaborated and described in details in previous papers [*Salamatin*, 1991; *Salamatin et al.*, 1994, 1995; *Salamatin and Ritz*, 1996]. The model is based on the study [*Salamatin*, 1991] of the ice sheet dynamics along a fixed flow line within the framework of shallow-ice approximation and with snow-firn-bubbly ice densification effects taken into consideration. General equations are examined and considerably simplified for the conditions prevailing in central Antarctica (Vostok Station) [*Salamatin et al.*, 1994, 1995]. They are presented in terms of reduced vertical distances z' measured from the bottom in ice equivalent and normalized by the local current ice sheet thickness Δ; that is, $Z = z'/\Delta$. The principal heat transfer equation is spatially one-dimensional but because of the normalization and an appropriate expression for the vertical particle velocity in the glacier body, it also partly accounts for horizontal advection effects, though neglecting temperature variation over the ice sheet surface. C. Ritz (personal communication) has confirmed the validity of such an approximation for the Antarctic Plateau, with its small geographical temperature gradients, by numerical tests. A special boundary condition on the upper surface of the ice sheet is formulated to describe the enhanced thermal resistance of the snow-firn stratum. Unlike the heat transfer

Table 1. Main Physical Parameters of the Heat and Mass Transfer Model for Vostok Station

Meaning of Parameters	Denotation	Basic Values*
Existence Conditions of the Ice Sheet		
Inversion temperature	T_i	$T_i^0 = -39°C$
Surface temperature	T_s	$T_s^0 = -57.9°C$/reference point/
Accumulation rate	b	$b^0 = 2.0$–2.8 cm/yr
Ice thickness/in ice equivalent/	Δ	$\Delta^0 = 3690$ m
Bottom fusion temperature	T_f	$-2.4°C$
Geothermal flux	q_0	0.050–0.056 W/m^2
Plastic-deformations − flow-rate ratio	σ	0–1
Distance from ice divide	s_0	120 km
Exponent factor of accumulation-rate variations	η_b	$0.112°C^{-1}$
Accumulation excess	e_b	0.25
Physical Properties of Pure Ice		
Density	ρ_0	920 kg/m^3
Specific heat capacity	$c(T)$	$c_0[1 + \alpha_c(T + 30)]$ $c_0 = 1.88$ kJ/(kg · °C) $\alpha_c = 0.004°C^{-1}$
Thermal conductivity	$\lambda(T)$	$\lambda_0[1 - \alpha_\lambda(T + 30)]$ $\lambda_0 = 2.55$ W/(m · °C) $\alpha_\lambda = 0.0044°C^{-1}$
Latent heat of fusion	L_f	333 kJ/kg
Glen-flow-law exponent	α	3.0

*Here superscript "0" denotes the present-day values of characteristics.

model previously employed by *Salamatin et al.* [1994, equations (6)–(8)], strain heating is explicitly included in the energy balance within the glacier body and is distinguished from the geothermal flux q_0 in the expression for the ice-melting rate w_0 at the ice sheet bottom.

Furthermore, velocity profiles written [see *Salamatin*, 1991] for the Glen ice-flow law were evaluated [*Salamatin et al.*, 1994, 1995] in accordance with *Lliboutry* [1979] and *Ritz* [1989, 1992]. The tuning parameter σ ($0 \le \sigma \le 1$) is introduced as a ratio between the partial ice-flow rate due to the shear strains and the total flow rate V, which includes ice sliding at the bottom. For the flow tube of the unit width, V is expressed as

$$V = s_0(1 + e_b)(b - \partial\Delta/\partial t), \quad (1)$$

where e_b is the mean relative excess of the accumulation rate in the central region of the ice sheet over the accumulation rate b at the site (Vostok) under consideration. The reduced distance s_0 from the ice divide (ridge B) in (1) is an apparent quantity which also takes into account the divergence of flow lines. Both factors s_0 and e_b can be estimated from the available geographical data [*Drewry*, 1983]. The main input physical parameters of the heat and mass transfer model and their basic values assumed for Vostok [see also *Salamatin et al.*, 1994, 1995] are presented in Table 1. Hereinafter the present-day values of characteristics are designated by the superscript "0".

To complete the above model, two additional submodels are necessary: one for predicting temporal variations of the accumulation rate b and another for simulating changes in the ice sheet thickness Δ (or surface elevation E). In accordance with *Robin* [1977], precipitation in Antarctica can be correlated to the water-vapor equilibrium pressure at the top of the inversion layer and, consequently, to the condensation (inversion) temperature. Certainly, the geographical distribution of accumulation rate is not solely governed by the local inversion temperatures but also depends on atmospheric circulation and wind scour, especially in the cold central regions where the precipitation is very low. However, the saturation vapor pressure and the inversion temperature represent the right tendency of temporal changes in the accumulation rate. Thus the past values b can be, at least approximately, calculated as today's local values b^0 corrected by the exponential factor, which is a function of the temperature δT_i counted from its contemporary level. The corresponding computational procedure was elaborated and described by *Ritz* [1989, 1992]:

$$b = b^0 \exp(\eta_b \delta T_i), \quad (2)$$

where η_b is the factor which accounts for all the precipitation mechanisms. In accordance with Ritz's estimations for the Antarctic Plateau, this parameter is mainly determined by the temperature dependence of water-vapor saturation pressure: $\eta_b = 6148.3/(273.15 + T_i^0)^2 \approx 0.112°C^{-1}$ at $T_i^0 = -39°C$ for Vostok Station.

The variations of surface elevation in the interior of the ice sheet represent, in general, the global response of the whole glacier to the changing climate and are not local by their nature. Special investigations conducted by *Salamatin and Ritz* [1996] revealed two major mechanisms that control this process: (1) the hydrodynamic interaction between a time-lagging low-accumulation-rate interior of a large ice sheet and its active high-accumulation-rate coastal zone and (2) the feedback between the temporal change in the inland surface elevation and the rate of the elevation growth. As a result, the evolution of the spatially averaged surface level in the central area of the ice sheet was described by a multitimescale nonlinear ordinary differential equation. Its parameters were estimated and verified for the Vostok region through the intercomparison with hydrodynamic predictions of the general model [*Ritz*, 1992]. The derived equation is now incorporated in our model instead of its high-frequency approximation used earlier by *Ritz* [1989] and *Salamatin et al.* [1994, 1995]. Consequently, the complete mathematical model of the heat and mass transfer in the ice sheet thickness becomes spatially quasi-local with the accumulation excess e_b relating the average mass balance in the interior regions to the local accumulation rate at Vostok.

Thus for any surface temperature $T_s(t)$ and inversion temperature variations $\delta T_i(t)$, being functions of time t, the temperature distribution $T(Z, t)$, the accumulation rate $b(t)$, and the ice sheet thickness $\Delta(t)$ are determined, provided that the model parameters (Table 1) are set up and tuned to the environmental conditions. The initial thermal state of the glacier is defined at a certain far moment t_0 (B.P.) in the past as a stationary state corresponding to the averaged surface temperature $\langle T_s \rangle$. The initial ice sheet thickness $\Delta(t = -t_0)$ is chosen so as to reach the present-day value $\Delta(t = 0) = \Delta^0$.

At the end of the model presentation it is important to point to the principal assumption underlying the above mathematical constructions and restricting their validity. That is the time invariant spatial patterns of accumulation rate and ice sheet flow which only make the fixed flow line theory acceptable. This may originally cause an additional uncertainty in the vertical velocities that could manifest itself first of all through the temporal change in the model parameters σ, s_0, e_b, and to a lesser degree in η_b. We discuss this point below in connection with the general problem of parametric sensitivity of inversion procedures.

A special interactive computer system is developed on the basis of the described model. (The computer code of the system for IBM-PC is available from the authors on request.) It is aimed at ice-core dating and palaeoclimatic reconstructions with the use of borehole temperature-depth profiles and isotope records. The sections of this paper actually follow the items of the main menu of this system.

3. Milankovich Cycles Remembered in the Vostok Borehole-Temperature Profile

The thermal diffusion within an ice sheet of finite thickness works as a "window" filter with respect to a surface temperature signal. Preliminary estimations [*Salamatin et al.*, 1994] show that in central Antarctica (Vostok) its frequency band corresponds to the main climatic cycles. The cut out temperature signal is nonlinearly transformed and remembered as the temperature-depth profile in the ice.

In this section we continue the line of the study by *Salamatin et al.* [1994]. The principal assumption made is that Milankovich astronomic cycles prevail [e.g., *Martinson et al.*, 1987; *Imbrie et al.*, 1992, 1993; *Waelbroeck et al.*, 1995] in the Pleistocene climate changes which are mainly responsible for the contemporary thermal state of the ice sheet [*Budd and Young*, 1983; *Dahl-Jensen and Johnsen*, 1986]. Hence the inverse problem may be formulated to infer the dominant "metronomic" part of local temperature history by fitting computed and measured borehole temperature profiles. To constrain the inverse procedure, we assume that the inferable components of the surface temperature oscillations $T_s(t)$ can be expressed as a sum of harmonics of Milankovich periods $t_1 = 100$, $t_2 = 41$, $t_3 = 23$, and $t_4 = 19$ kyr:

$$T_s(t) = \langle T_s \rangle + \sum_{i=1}^{4} [A_i \cos(\omega_i t) - B_i \sin(\omega_i t)], \qquad (3)$$

$$-t_0 < t < 0,$$

where frequencies $\omega_i = 2\pi/t_i$ are fixed and only the amplitudes (and the phase lags) A_i, B_i ($i = 1, \cdots, 4$) are to be found. Hereinafter the value t_0 is taken as $t_0 = 3t_1 = 300$ kyr.

As for the inversion temperature perturbations, an approximate simplified relation is assumed at this step, after *Jouzel et al.* [1987]:

$$\delta T_i / \delta T_s = C_t, \qquad \delta T_s = T_s(t) - T_s^0 \qquad (4)$$

with the factor $C_t = 0.67$. A more general form of this equation is suggested and used in section 5.

Discrepancy between the computed present-day temperature profile $T(Z, t = 0)$ and an experimental temperature $T_{ex}(Z)$ observed in a deep borehole is estimated as the mean square (standard) deviation S. Thus the inverse procedure is reduced to minimizing the target function S as a function of A_i, B_i ($i = 1, \cdots, 4$) at given values of $\langle T_s \rangle$, C_t, and the other model parameters (see Table 1): b^0, q_0, σ, $\cdots$.

We recognize that both the initial basic assumption and the above inverse procedure are somewhat limiting. Following general conceptions of Milankovich theory [*Imbrie et al.*, 1992, 1993], they imply a quasi-linear response of Earth's climate to orbital forcing, disregarding "climatic noise," with fixed constant frequencies and phase shifts (supposed to be determined) in the metronomic part of local palaeotemperature oscillations given by (3) and (4). The latter step is an approximation even in the framework of Earth astronomy [*Berger*, 1978] and is supposed to be valid only within a relatively short interval of cosmic history not exceeding several recent glacial-interglacial cycles. Another peculiarity is linked with the introduction of the 100-kyr eccentricity period into eq. (3). This radiation astronomic cycle is thought to be too small in amplitude and too late in phase to produce the corresponding temperature cycle by direct forcing, although there are various plausible explanations of its even dominant presence in global climate changes, which are reviewed by *Imbrie et al.* [1993]. Indeed, the computational tests discussed below prove that such a harmonic with a period t_1 at least close to 100 kyr is present in the borehole temperature record. Furthermore, it is clear that, for each of the harmonic components, which can be revealed in the surface temperature variations, the borehole temperature mostly reflects their recent periods (see analysis at the end of this section) and any use of expansion (3) at greater times is a mere periodic extrapolation. Nevertheless, we still hope that the main climate changes might be predicted and dated and that the set of trigonometric functions in (3) can be regarded as an appropriate mathematical basis to expand the dominant part of $T_s(t)$.

Since the beginning of the deep drilling program at Vostok Station in 1970, a number of temperature surveys [*Vostretsov et al.*, 1984; *Barkov et al.*, 1989; *Salamatin et al.*, 1994] have been performed to a depth of about 2000 m in different boreholes. All experimental profiles are very close. Here we use the most accurate data [*Salamatin et al.*, 1994] obtained by Yu. Rydvan (St. Petersburg Mining Institute) in the 3G hole in 1988, three years after the drilling operations had been stopped. The absolute error of the measurements, originated primarily from a systematic error of the calibration procedure, was estimated to be about ±0.05°C (R. N. Vostretsov, personal communication). This type of error could induce a shift in the experimental temperature profile rather than a false wave-like signal detectable by the inverse procedure. The temperature logging was performed 3 times within 6 months in the fluid-filled part of the borehole. Each time, the temperatures were acquired while both lowering down and pulling up the sensor, with four or five readings at each depth. The reproducibility was found to be 0.005° ÷ 0.01°C, while the sensitivity of the measuring system was much higher. The estimated variance of the mea-

surements is thought to represent the mismatch between temperatures in the borehole and in the surrounding ice, in particular due to the logging activities. The latter source of errors causes the main uncertainty in the palaeoclimatic reconstructions discussed below.

Another temperature profile was measured by A. Volkov (St. Petersburg Mining Institute) in the 2755-m deep 5G hole in 1993, six months after the thermal-drilling operations had been stopped. The new data cover mainly the bottom part of the borehole below a depth of 1950 m. These measurements are not used in our study because their accuracy, as shown below, appears to be much lower than that of the basic surveys in 1988. However, the inverse procedure was tested on the stacked experimental temperature-depth curve continued to the 2750 m depth to verify the consistency of our palaeoclimatic reconstructions and their sensitivity to the temperature profile extension.

Since the model was improved and the time range of the palaeoreconstruction extended to 250 kyr B.P., almost all computational tests performed by *Salamatin et al.* [1994, 1995] were repeated anew. Preliminary estimates for the mean surface temperature, $-63.5 < \langle T_s \rangle < -62.3$°C derived from the stacked 2755-m isotope record (see sections 4, 5), appeared somewhat different from those assumed in the earlier papers. In spite of this, all previous conclusions are confirmed, and the principal one remains the same: although the inferred palaeotemperature oscillations in diverse computational runs may vary in amplitudes of their harmonic components, the major climatic events (peaks and troughs) and their ages are always reliably reproducible.

The main results of the metronomic signal reconstruction for different limiting cases are brought together in Figure 1a. These series of computational tests were performed, with model parameters given in Table 1 at fixed $\langle T_s \rangle = -62.9$°C for $\sigma = 0$ and 1, to estimate the sensitivity of the inverse procedure to the ice sheet flow scheme: with no shear strain in the glacier body or without ice sliding on the bedrock, respectively. In the first situation, two possible hydraulic regimes should be distinguished. One is the case when the water produced by melting at the bottom of the ice sheet can freely run off or penetrate into the underlying rocks without substantial accumulation in the basal layer. Another concerns the formation of a subglacial lake when the meltwater is locked under the ice thickness and the melting process stops due to the enhanced thermal resistance at the bedrock-ice interface containing the water layer. In accordance with *Ridley et al.* [1993]

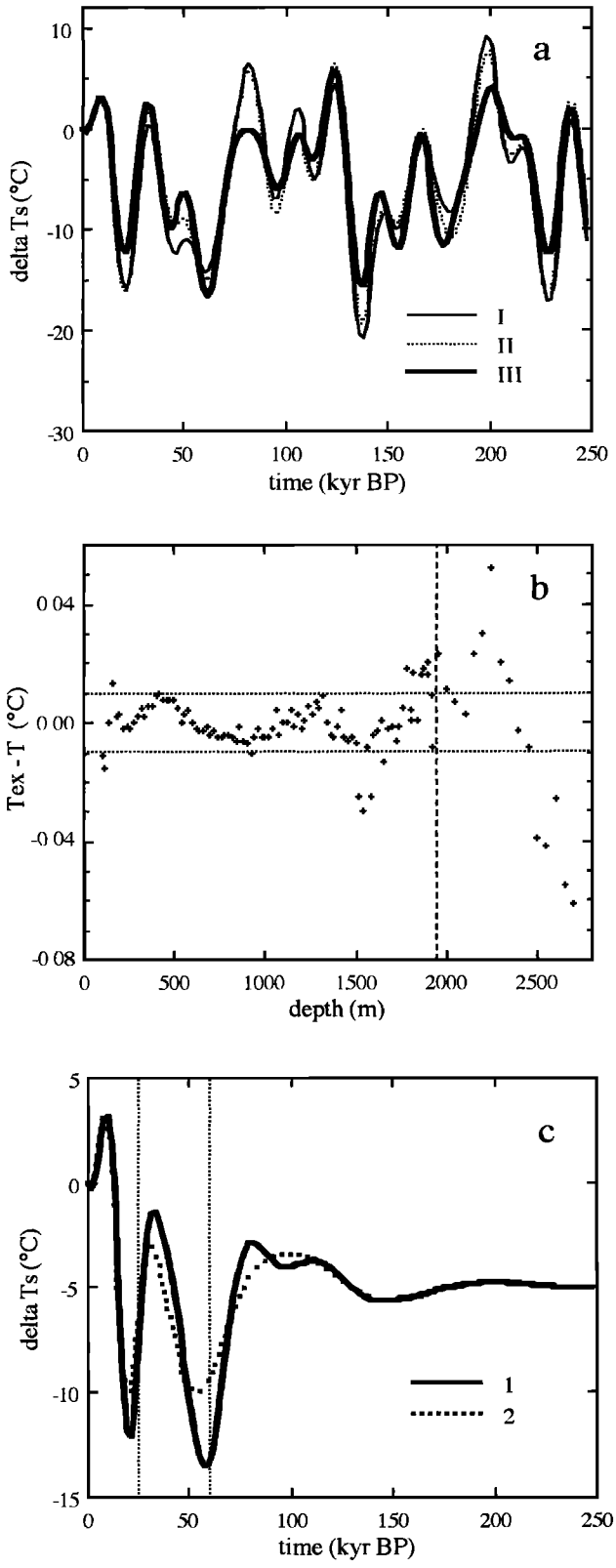

Figure 1. (opposite) (a) Metronomic signal in the Vostok surface temperature variations inferred from borehole temperature profile under different plausible conditions at the ice sheet bottom: (curve I) basal sliding ($\sigma = 0$) with free drainage of meltwater, (curve II) basal sliding ($\sigma = 0$) over a subglacial lake; (curve III) nonsliding conditions ($\sigma = 1$). The temperature variations δT_s are reported with respect to the reference point $T_s^0 = -57.9$°C. (b) Discrepancy between computed (T) and observed (T_{ex}) temperatures within the ice sheet. The vertical dashed line separates measurements in the 3G hole from those in the 5G hole. The horizontal dotted lines bound a mean standard deviation (0.01°C) of the measurements in the 3G hole. (c) The extinguishing signals of the surface temperature history (variant III in Figure 1a) reliably remembered at the two sensitivity levels of the borehole temperature prediction: 0.01°C (1) and 0.05°C (2). The dotted boundaries at 25 and 60 kyr are the sensitivity thresholds for the precession and longer-period (obliquity and radiation) Milankovich cycles, respectively. The simulated borehole temperature profile responds by mean deviation of 0.01°C if the components of the metronomic signal are degraded back through time starting from these thresholds.

and *Kapitsa et al.* [1996] the latter case seems to be rather plausible for Vostok and can formally be modeled [*Salamatin et al.*, 1994] if the value of the latent heat of ice fusion L_f is taken large (tends to infinity), resulting in zero bottom-melting rates ($w_0 \to 0$). The probable ranges (see Table 1) of the present-day accumulation rate b^0 and geothermal flux q_0 were also scanned, and thus the latter quantities were treated as free parameters in the inversion procedure.

In the two cases for $\sigma = 0$, the best fits of the simulated temperature profiles to the experimental one with $S = 0.0075$°C are found at $q_0 \approx 0.053$ W/m^2 and at definite values of b^0:

(I) $b^0 = 2.1$ cm/yr

$A_1 = 6.006$, $A_2 = 4.944$, $A_3 = -4.054$, $A_4 = -1.886$°C

$B_1 = -1.358$, $B_2 = -2.404$, $B_3 = 1.001$, $B_4 = -1.414$°C

(II) $b^0 = 2.2$ cm/yr ($L_f \to \infty$)

$A_1 = 4.631$, $A_2 = 6.083$, $A_3 = -3.998$, $A_4 = -1.710$°C

$B_1 = -0.192$, $B_2 = -1.661$, $B_3 = 0.792$, $B_4 = -1.622$°C

The corresponding palaeotemperature oscillations $T_s(t)$ are shown in Figure 1a by curves I and II. It should be noted that for $\sigma = 0$, internal shear-strain and ice-sliding (friction) heating becomes zero. On the contrary, for $\sigma = 1$, the dissipation of mechanical energy within the basal layer of the ice sheet results in inverse proportionality between the best-fit values of q_0 and b^0. For instance, the increase in b^0 from 2.4 to 2.8 cm/yr leads to a slight change in q_0 from 0.053 to 0.052 W/m^2 which slows down the bottom melting rate to maintain the same optimal balance of the internal energy in the glacier. The values of S vary within the range 0.0072°–0.0073°C. The same conclusion was derived by *Ritz* [1989].

The surface temperature-time curve inferred at $\sigma = 1$ for the upper bound of the present-day accumulation rate at Vostok [*Lorius et al.*, 1985; *Jouzel et al.*, 1993; *Barkov and Lipenkov*, 1996] corresponds to $q_0 \approx 0.053$ W/m^2 and is specified by

(III) $b^0 = 2.6$ cm/yr

$A_1 = 4.252$, $A_2 = 4.428$, $A_3 = -2.530$, $A_4 = -1.155$°C

$B_1 = 1.502$, $B_2 = -1.188$, $B_3 = 1.958$, $B_4 = -2.404$°C

It is depicted as curve III in Figure 1a.

The best-fit value of the geothermal flux q_0 is in a good agreement with the general prediction of $q_0 \approx 0.054$ W/m^2 for the central part of the Antarctic ice sheet obtained from analysis of the thermal regime above subglacial lakes at more than 50 locations [*Seigert and Dowdeswell*, 1996]. The present-day accumulation rate at Vostok $b^0 \approx 2.4$ cm/yr [*Barkov and Lipenkov*, 1996] falls exactly between the two limiting cases II and III.

The experimental temperature profile used in the inverse procedure is not perfect and all reconstructed surface temperature signals, which provide simulated present-day temperatures in the ice thickness within the error range of measurements, could be equally valid. Hence we would have to present not only the definite best-fit sets of the harmonic amplitudes in (3) but the corresponding regions in the parametric space. On the other hand, the coefficients A_i, B_i ($i = 1, \cdots, 4$), which would satisfy such limitations, appear to be closely interrelated and their values form complicated hypersurfaces in the eight-dimensional (8-D) space. Admissible selective variation of any free coefficient (while others are fixed) in (3) does not exceed 1% within the 0.01°C bounds of the S-function deviation. However, the resulting sum (3) remains very stable, even if the harmonic amplitudes change noticeably. Therefore it is relevant to evaluate the uncertainty of the inverse procedure by direct comparison of extreme samples among the deduced metronomic signals. The three described versions of the past surface temperature variations answer to this purpose: all other acceptable solutions fall within the range bounded by the three curves. These variants will be referred to hereinafter as I, II, and III, respectively. Figure 1a evidently confirms the time stability of the main inferred climatic events. The variance in ages of single peaks and troughs in these metronomic signals does not exceed 1.5 kyr and is estimated to be about 0.65 kyr on average.

The variants I, II, and III cover all plausible extreme situations of the environmental conditions prescribed by the model parameters in Table 1. Notice that the apparent distance s_0 from the ice divide manifests itself through the internal strain heating and renders the same effect as σ. The latter parameter is also a key one in the ice velocity profiles [*Salamatin*, 1991; *Salamatin et al.*, 1994, 1995] and their maximal transformations take place within the interval $0 \le \sigma \le 1$. Accumulation excess e_b in (1) and the exponent factor η_b in (2) influence only through the submodels for b and Δ, which extreme cases were tested earlier by *Salamatin et al.* [1994] and did not change the estimations. Furthermore, any variations of η_b are equivalent to the reciprocal changes of the ratio C_t defined by (4). The sensitivity of the metronomic signals to a plausible choice of this parameter is discussed below.

Next, it is worth noting that in all three cases I, II, and III, the 100-kyr period is well distinguishable and comparatively significant, although not dominant. Computations show that this term cannot be excluded from (3) without losing the accuracy level in the model representation of the borehole temperature profile as well as the general resemblance between the inferred surface temperature variations and the isotopic temperature record. Nevertheless, 10% uncertainty may be prescribed for the frequency ω_1 (i.e., for the period t_1) of the first harmonic in (3), due to the possible indirect response of the Earth climate to the radiation astronomic cycle [e.g., *Jouzel et al.*, 1987].

Additional errors in the climate event timing are linked to the sensitivity of the palaeoreconstructions to the parameters C_t and $\langle T_s \rangle$ in (2)–(4). Although $C_t = 0.67$ [*Jouzel and Merlivat*, 1984] is regarded here as a reliable average value, the lower estimate ($C_t = 0.44$) has been established from the linear relationship between the inversion strength $T_i - T_s$ and surface temperature T_s observed at Vostok in 1958 [*Phillpot and Zillman*, 1970]. The changes in the inversion-surface temperature ratio influence model predictions for the accumulation rate in (2)–(4). As it has already been mentioned, the mean Pleistocene temperature $\langle T_s \rangle$ may vary within the range −63.5° to −62.3°C.

All these ranges of the parameters ω_1, C_t, and $\langle T_s \rangle$ have been tested in a special series of computations which fully confirm the principal conclusion: every time the inferred metronomes provide the same best-fit level of the standard deviation $S \sim 0.007$°–0.0075°C between simulated and measured borehole temperature profiles, they remain similar in shape to the basic variants I–III shown in Figure 1a and keep qualitative resemblance to the isotopic temperature record.

These computational experiments present a family of metronomic signals with nonuniformly distributed uncertainties in positions of their extrema. Maximal deviations in ages of the climatic events, which may result from the changes in ω_1, C_t, and $\langle T_s \rangle$, do not exceed ± 3 kyr. A sort of "nodal" region can be distinguished each 40–60 kyr with minimal uncertainties of ± 1 kyr in peak positioning, while the average age variance is about 1.25 kyr. Thus the standard error in dating peaks and troughs in the inferred metronomes can be estimated as 1.5 kyr. We continue this analysis in the next section to take into account additional sources of uncertainties which influence the ice core dating procedure.

To test the stacked 2550-m long borehole temperature profile, the mean values of $b^0 = 2.4$ cm/yr and $\sigma = 0.5$ were used at $q_0 \approx 0.053$ W/m^2. The best-fit surface temperature oscillations are indistinguishable from curve III in Figure 1a. The difference between simulated and observed temperatures is shown in Figure 1b. The standard deviation S for the upper part of the profile to 1920 m (3G hole) is comparable with the above estimates, while for the deeper measurements (5G hole) it is almost 4 times higher: $S = 0.03$°C. Thus theoretical predictions remain in full agreement with the new observations within the limits of their accuracy, but yet the use of the basic experimental profile [*Salamatin et al.*, 1994] was obviously preferable.

In all computations the present-day mean surface temperature is identically found as $T_s^0 = -57.9$°C, which seems to be a very reliable estimate. The difference between the latter value and meteorological observations of the present-day mean surface-air temperature: −55.5°C at Vostok [*Jouzel et al.*, 1987; *Barkov and Lipenkov*, 1996] is quite obvious. This is an evidence that the ice sheet surface temperatures and the near-surface air temperatures must be distinguished.

Finally, we should point out a crucial difference between the recent part of the inferred surface temperature oscillations remembered by the borehole temperature profile and their older part which is constrained by the assumption about the Milankovich periodicity determining the climate. To reveal the sensitivity thresholds for the harmonic components in (3), we selectively and gradually degraded their amplitudes A_i, B_i ($i = 1, \cdots, 4$) back through time, starting from a certain "switch" moment. To do this, we used exponential factors for which fading rates were prescribed by the relaxation timescales equal to the halves of the respective harmonic periods. The extinguishing signals shown in Figure 1c were calculated as for variant III. They provide the simulated borehole temperature profiles with accuracy of ±0.01°C (curve 1) and ±0.05°C (curve 2) with respect to the measurements. Notice that the 0.01°C sensitivity level is exceeded when the "switch" is set at 1, 1.5, and 0.5 periods before present for precession, obliquity and radiation cycles, respectively. The 25 kyr and 60 kyr bounds shown in Figure 1c by vertical dotted lines are, thus, considered to be the sensitivity thresholds for the precession and longer-period Milankovich cycles, respectively. Although the recent (20–25 kyr) history of the precession signal is reliably remembered in the Vostok borehole temperature profile, this high-frequency component of the surface temperature fluctuations does not render any significant perturbations to a deeper part of the ice sheet below 1500 m. The past precession oscillations faded from the borehole temperature memory and the amount of belief in their high swings revealed in the metronomic curves should be reduced to minimum. The obliquity cycle is 2 times longer and appears to be much stronger in amplitude. Because

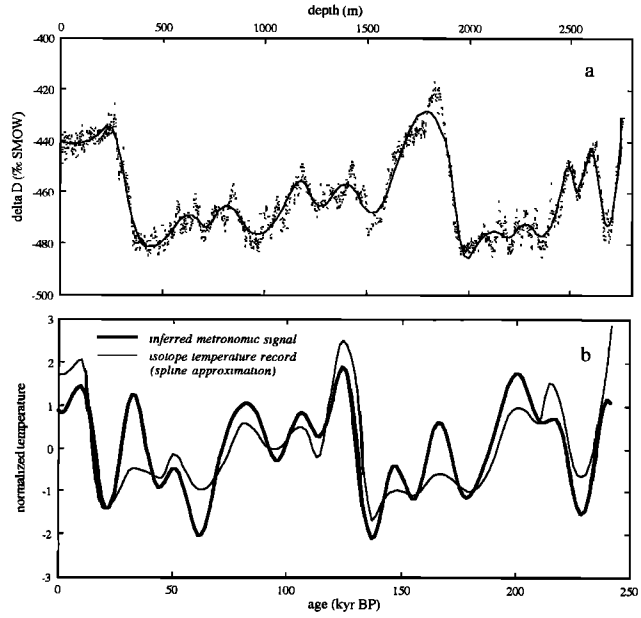

Figure 2. Dating of the Vostok isotope record by its correlation with the metronomic signal inferred from temperature profile in the ice sheet. (a) The stacked Vostok deuterium profile (dots) and its parabolic-spline approximation (solid line) adjusted to facilitate the correlation procedure. (b) The smoothed isotope record (thin line) correlated with the metronome (bold line) corresponding to variant III in Figure 1a.

of the low accumulation rates its full recent period and the end of the previous one are preserved in the ice temperature memory in central Antarctica. The latter signal is filtered and still well distinguished in the bottom part of the Vostok temperature profile. At the same time, it is quite clear that the 100-kyr cycle is too long to be entirely recorded within the 2000 m of the ice-sheet thickness. The above analysis gives us a basis for constraining the ice core timescale and interpreting the results of the isotopic palaeothermometer calibration.

4. Vostok Ice Core Chronology

Now, when the local geophysical metronome for Vostok is established, the next step is to correlate it with an isotopic temperature record to deduce ice core timescale.

The deuterium content (δD) of the Vostok ice cores from the deep boreholes 3G (2083 m) and 4G (2546 m) was studied by *Jouzel et al.* [1987, 1993]. Recently, a new set of isotopic data from the 5G core has become available [*Jouzel et al.*, 1996]. The stacked continuous deuterium-depth profile to 2755 m, which we use further for ice core dating and palaeoclimatic analysis, is plotted by dots in Figure 2a.

The conventional empirical relationship between deuterium ratios and inversion-temperature fluctuations, supported by modeling [*Dansgaard*, 1964; *Robin*, 1977; *Jouzel and Merlivat*, 1984], can be written in the following general form:

$$\delta T_i = (\delta D - 8\delta^{18}O_{sw})/C_T, \qquad (5)$$

where the term $8\delta^{18}O_{sw}$ is the correction of δD for past changes in the oxygen-isotope composition of ocean water, and C_T is the coefficient estimated by *Jouzel et al.* [1987, 1993] as $C_T = 9$ per mil/°C. Hereinafter a parabolic-spline approxima-

Table 2. Vostok Ice Core Chronology: Age-Depth Correlation of Peaks and Troughs in Metronomic and Isotopic Temperature Signals and Standard Errors of the Correlation

Depth, m	Age, kyr	Error, kyr	Depth, m	Age, kyr	Error, kyr
52	1.7*	1.9	1782	123.9	1.1
218	8.4	1.5	2005	137.9	1.9
444	21.5	1.6	2123	149.3	2.8
626	33.2	1.2	2186	154.5	1.4
708	45.9	2.8	2277	167.1	1.0
816	50.5	1.2	2355	180.7	3.3
970	61.3	2.0	2489	199.6	3.9
1172	82.0	3.3	2533	212.1	2.9
1275	95.5	3.8	2593	215.6	1.5
1392	106.0	3.2	2680	228.9	1.0
1525	113.8	1.8	2760	241.4	...

*This value corresponds to the metronomic record III.

tion of the $\delta^{18}O_{sw}$ variations, obtained by *Sowers et al.* [1993] versus SPECMAP ages, is used in (5).

To deduce the ice core chronology we assume that although (4) relating δT_s and δT_t may be approximate or even too much simplified, the surface and inversion temperatures underwent main climatic changes synchronously, and therefore the smoothed isotopic temperature record is supposed to mimic the inferred metronomic signal. Thus we have to filter out high-frequency components of the isotopic record δD in (5) and then identify maximums and minimums of the smoothed palaeoclimatic signal $\delta D - 8\delta^{18}O_{sw}$ with those of the inferred metronomic part of δT_s given by (3). To do this, a mean square parabolic-spline approximation was applied to the deuterium record. Spline nodes were chosen approximately as midpoints between the major climatic events (peaks and troughs) on the depth scale. The resulting curve used in this study is shown by the solid line in Figure 2a.

Obviously, such an approximation is not determined uniquely, and the tuning of the extrema depends on spline-nodes positioning. This uncertainty was estimated in a special series of computational (sensitivity) tests by shifting the nodes. Another source of possible errors comes from the correction for the change in the mean isotopic composition of ocean water, which, though comparatively small, causes additional perturbations when the original deuterium record is interpreted in terms of the inversion temperature variations (see equation (5)). This correction in the ice-core dating procedure was performed iteratively; however, we include it into the depth-error range because neither the deduced timescale nor the SPECMAP chronology [*Martinson et al.*, 1987] are absolute. The depths of maximums and minimums on the smoothed isotopic curve are given in Table 2. Maximal errors in their positioning do not exceed ±15 m, and on average the total variance is about 9 m, which makes not more than 0.8 kyr in age. The mean ages of the corresponding climatic events revealed in the metronomic temperature signals (variants I–III) are also presented in Table 2. As has been shown in section 3, the average uncertainty in their determination is about 1.5 kyr. Thus the standard error of the peaks-and-troughs correlation procedure is about 1.7 kyr.

The upper 100- to 200-m layer is relatively the most uncertain both because of the comparatively small ages of the firn-ice deposits and because of the rather high dispersion of the deuterium-content measurements (see Figure 2a) in this part of the record. For this reason the star-marked value in Table 2 is taken as it was determined in the surface temperature reconstruction for variant III, since the latter estimate is close to the EGT time scale predictions which are undoubtedly much more reliable in the shallowest part of the ice sheet thickness.

In order to obtain a continuous timescale we admit the linear dependence of age on depth between each pair of neighboring peaks and troughs in the ice core chronology given by Table 2. Thus it becomes possible to compare the inferred ice sheet surface palaeotemperature variations with the smoothed isotopic temperature record quantitatively. The correlation coefficients (r^2) are found to be rather high: $r^2 = 0.71$, 0.75, and 0.80 for variants I, II, and III, respectively. The best correlation variant is shown in Figure 2b along with smoothed isotopic temperature record (both curves are normalized). Figure 2b evidently illustrates coincidence in positions of the inflection points on these signals initially fitted only by peaks and troughs. This means that the dating procedure is not sensitive (at least within the limits of the estimated accuracy) to a choice of climatic events which are used to correlate the isotopic record and the geophysical metronome. In spite of the resemblance between the two curves the difference mainly in the precession components should be noted, although in accordance with the sensitivity tests performed in section 3, this discrepancy cannot be considered as a fact of any quantitative meaning.

The resulting Vostok timescale as a compound of linear interpolations is presented in Figure 3a and is referred to hereinafter as Geophysical-Metronome Timescale (GMTS). The distribution of the total correlation errors is presented in Table 2. It clearly reveals the alternating regions with high and low error levels of the correlation procedure.

The above discussions on the uncertainties of the ice core dating would not be complete if we did not take into account the errors linked to the principal assumptions on which the formulation and the use of metronome (3) are based (see section 3). Mainly, they are the linear response of the climate to orbital forcing and the extrapolation of expansion (3) beyond the time range of the borehole temperature memory. Physically, this results in the so-called overtuning effect [*Martinson et al.*, 1987] due to neglecting nonlinearity in climatic transfer mechanisms (climatic noise) [*Imbrie et al.*, 1992]. For obliquity (41-kyr cycle) and precession (23-kyr cycle) components in (3) primarily responsible for the metronome extrema the corresponding errors were estimated to be not more than ±2.5–3.5 kyr by *Martinson et al.* [1987] and less than ±4 kyr by *Imbrie et al.* [1992]. Consequently, combining the latter values and the correlation error estimate, 1.7 kyr, we can predict the total average accuracy of the ice core chronostratigraphy (Table 2) as ±3.0–4.5 kyr. The distribution of the overall uncertainty of the dating along the ice core is shown with error blanket in Figure 3a.

The difference in ages between EGT [*Jouzel et al.*, 1993] and GMTS is drawn in Figure 3b by the solid line. As it was stated earlier [*Salamatin et al.*, 1994], the significant discrepancy (exceeding 4–5 kyr) between the two chronologies was observed for the large depth only (below 1800–1900 m) and reached almost 20 kyr at the level of 2760 m, what was within the EGT error range [*Jouzel et al.*, 1993]. We discuss the conditions which eliminate this deviation in section 6 in the context of the isotope-temperature transfer function and spatial variations of the accumulation rate upstream of Vostok. The new ice age-

depth correlation does not differ much from the recent results obtained by *Waelbroeck et al.* [1995] on the basis of tuning the Vostok deuterium record to the insolation time curve. The standard deviation between the two timescales is about 4.8 kyr.

GMTS agrees well with an independent "marine" timescale derived for Vostok [*Pichon et al.*, 1992] to a depth of 2000 m through direct correlation of the ice core isotopic temperature record [*Jouzel et al.*, 1987] with the sea surface temperature (SST) reconstructed from fossil Antarctic diatoms. Pichon's ice age estimates (their differences from EGT) are shown by squares in Figure 3b, displaying the standard deviation of about 2.8 kyr from the GMTS age predictions. This is in full agreement with analogous dating by *Shackleton et al.* [1992] (not shown). A common temporal framework for Vostok ice cores and deep sea cores was developed by *Sowers et al.* [1993] through correlating the $\delta^{18}O$ record of atmospheric O_2 from air bubbles trapped in the ice to the $\delta^{18}O$ of sea water. The ice age was calculated from the age of the atmospheric air in accordance with *Barnola et al.* [1991]. The mean square discrepancy between our chronology (Table 2) and the correlated "oceanic" ice ages is about 3.4 kyr.

Another possibility to compare the Vostok ice age-depth curve and the marine (SPECMAP) timescale is to use the dust markers [*Petit et al.*, 1990]. It is based on the assumption that the Antarctic dust records and analogous dust-proxy signals in deep sea cores from different geographic areas (and even hemispheres) may be comparable. However, since dust stages (their abrupt starts and ends) could be out of phase from one place to another due to the difference in local short-term climatic histories, we suggest here that only maximum peaks in dust accumulation rates might globally be more in phase. This is because they correspond to fully developed glacial conditions for which dust mobilization and long-range transport likely had a general character (with accuracy not worse than ±5 kyr), while the start-and-end dust events could be more linked to the regional conditions. So we compare the stacked 2755-m record of the dust-volume accumulation rate at Vostok [*Jouzel et al.*, 1996] and the mass accumulation rate of lithogenic sediments in the northwest Arabian Sea [*Clemens and Prell*, 1990]. To reach maximal reliability in dating, only the four most obvious major peaks in the two records are identified. They correspond to the Vostok ice depth levels of about 420, 970, 2120, and 2650 m and to the SPECMAP ages of 22.3, 62.8, 150.4, and 228.6 kyr, respectively, which is very close to the ice age predictions based on the geophysical metronome: 20.1, 61.3, 149.0, and 224.3 kyr (see Table 2). These data are presented in Figure 3b by triangles. All different estimates of the Vostok ice age discussed above and deduced from correlations with "oceanic" signals fall exactly within the range of the general tuning uncertainties (±2.5–3.5 kyr) of the SPECMAP chronology. However, they are in some way or other linked to the Milankovich conception of the orbitally driven climate and cannot be regarded as completely independent.

It is important to note that to compare the metronome with the isotopic temperature (deuterium) record and to deduce the ice core timescale, we do not need to know the magnitude of the coefficient C_T in (5), i.e., the isotope-temperature temporal slope. Hence we can calibrate the latter relationship now by fitting the present-day temperature-depth curve computed for isotopic surface temperature to the borehole temperature measurements.

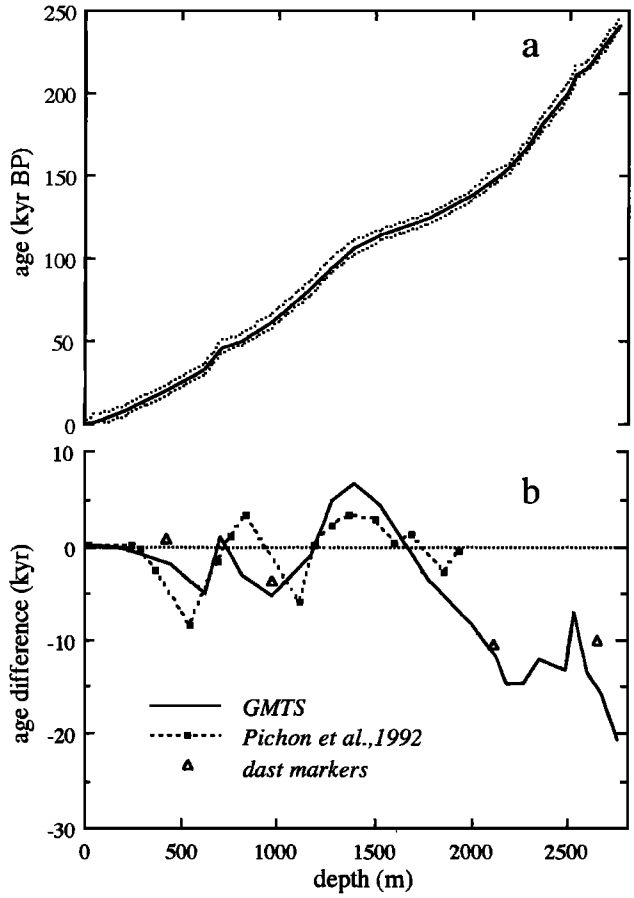

Figure 3. (a) Age-depth relation for the Vostok ice core (GMTS). The error blanket indicates overall uncertainties of the dating procedure. (b) Age difference between EGT and other chronologies suggested for the Vostok ice core (see text).

5. Isotopic Paleothermometer Calibration

The primary step in matching the inversion temperature variations δT_i, determined by (5), with observed borehole temperature is to relate δT_i to the ice sheet surface temperature δT_s which is the principal input parameter of the heat-and-mass-transfer model.

It is clear that during a full palaeoclimatic cycle such a relation may be not just a direct proportionality between δT_i and δT_s. First of all, one should take into account that both temperatures are influenced by local (counted from the present-day state) changes δE in the ice sheet surface elevation above see level. Let us accept (4) deduced by *Jouzel and Merlivat* [1984] from geophysical atmospheric observations in Antarctica as an original equation valid for the present-day conditions. Let α_{Ti} and α_{Ts}, be the inversion and surface temperature-elevation gradients at the site. Then for nonzero δE this relation may be rewritten in the following form:

$$\delta T_i - \alpha_{Ti}\delta E = C_i(\delta T_s - \alpha_{Ts}\delta E). \quad (6)$$

Equation (6) implies that in the general case the inversion strength may differently depend on surface temperature variations induced by the surface elevation and by climate changes, which seems unlikely. It would not be so if we assumed that geographical and temporal fluctuations of the surface temperature had the same impact on the inversion temperature, put-

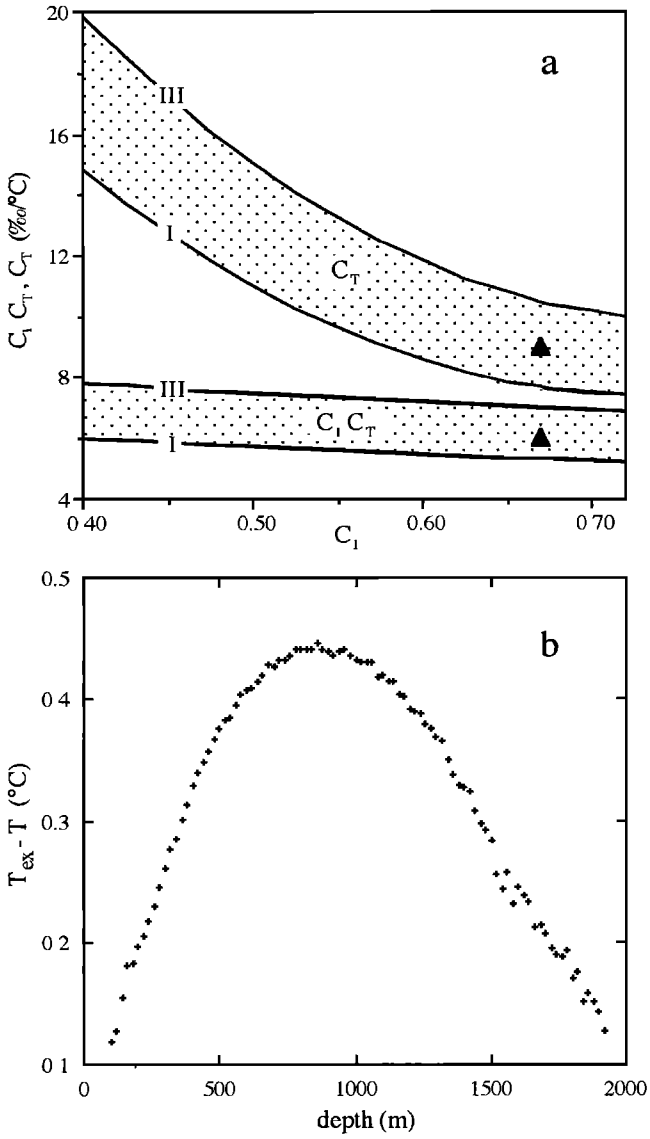

Figure 4. (a) Regions of the best-fit parameters C_T and C_tC_T in equations (5) and (8) versus C_t. The bounds correspond to the limiting cases I and III. The conventional estimates based on geographical data are shown by triangles. (b) The mismatch between measured and simulated (variant III at $\delta_p \equiv 0$) borehole temperature profiles. The produced curve is considered as a thermally transformed δ_p signal remembered in the ice sheet thickness.

ting $\alpha_{Ti} \approx \alpha_{Ts}C_i$. Here we do not constrain our consideration to the particular case when $C_t = 0.67$ and regard this coefficient as a tuning parameter, using reasonable estimates for α_{Ti} and α_{Ts} to show that the influence of δE (if it exists) is small.

We assume further that the sea level variations are inversely proportional to continental ice volume fluctuations and are equal to $\alpha_L\delta^{18}O_{sw}$, where $\alpha_L < 0$ is a constant factor. Consequently, we obtain

$$\delta E = K_t\delta\Delta - \alpha_L\delta^{18}O_{sw}. \quad (7)$$

Here K_t is the isostasy coefficient approximately determined for hydrostatic ice-rock equilibrium as $K_t = 1 - \rho_0/\rho_r$, and ρ_r is the density of the bedrock. Such simplification was justified for the central part of Antarctic ice sheet by *Salamatin and Ritz* [1996] on the basis of computational simulations by *Le Meur and Huybrechts* [1996].

Finally, combining the above equations (6) and (7), we come to the following possible generalization of the basic equations (4) and (5):

$$\delta T_s = \frac{\delta T_i}{C_i} - \frac{\alpha_{Ti} - \alpha_{Ts}C_i}{C_i}(K_t\delta\Delta - \alpha_L\delta^{18}O_{sw})$$

$$= \frac{\delta D - 8\delta^{18}O_{sw}}{C_tC_T} - \frac{\alpha_{Ti} - \alpha_{Ts}C_i}{C_i}(K_t\delta\Delta - \alpha_L\delta^{18}O_{sw}). \quad (8)$$

Assuming approximately $\alpha_{Ti} \approx \alpha_{Ts} = \alpha_T$, at Vostok Station we take, after *Aver'yanov* [1988], $\alpha_T = -0.01$°C/m. Furthermore, we also estimate $\alpha_L \approx -100$ m/per mil and $K_t = 0.66$ ($\rho_0 = 920$ kg/m^3, $\rho_r = 2700$ kg/m^3). Thus using the sea water isotopic composition determined by *Sowers et al.* [1993] and the ice sheet thickness variations simulated by *Salamatin and Ritz* [1996], it is easy to conclude that the contribution of $\delta\Delta$ and $\delta^{18}O_{sw}$ perturbations in (8) is relatively small and does not exceed 0.5°C, i.e., 5% of the expected surface temperature fluctuations δT_s. Hence the first term in (8) containing the two factors C_t and C_T in a single product is undoubtedly a leading one and the influences of these parameters on δT_s are almost indistinguishable. However, C_T manifests itself additionally (although not dominantly) in accumulation rate predictions as a combination C_T/η_b through (2) and (5). As a result, our strategy in calibrating isotopic palaeothermometer is twofold: (1) to adjust the factor C_T in (5) (i.e., the product C_tC_T in (8)) at plausible values of C_t and (2) to test the validity of (8) in order to make further appropriate corrections in case of necessity. It is clear that the desired calibration will be constrained by the borehole temperatures only within the recent time interval which does not exceed 60 kyr (see Figure 1c and discussion in section 3).

In order to calculate the absolute ice sheet surface temperature $T_s(t)$ and to run the heat-and-mass-transfer model, we need to complete (8) with the contemporary mean annual surface temperature value T_s^0 which is taken hereinafter to be equal to −57.9°C (see section 3). Besides, the temperature history documented in the deuterium record covers only the last 240 kyr, and in the computational procedure we extended it to the past (300 kyr BP) by metronomic signal inferred in section 3.

Preliminary series of calculations were performed with the smoothed isotopic record (see Figure 2a) in (5) and (8) for all limiting situations (at $\sigma = 0$ and 1) considered in section 3 and for different values of C_t from 0.44 [*Phillpot and Zillman*, 1970] to 0.67 [*Jouzel and Merlivat*, 1984]. The parameter C_T was tuned so as to minimize the standard deviation S between the computed present-day temperature profile and the borehole temperature measurements. The best-fit values of the product C_tC_T in (8) remained comparatively stable: 6.5 ± 1.5 per mil/°C. The contour plots of the minimal values of the target function are presented in Figure 4a as C_T and C_tC_T diagrams versus C_t. It should be pointed out that both C_T and C_tC_T decrease when C_t increases. Hence smaller values of the product C_tC_T can be explained only by a drop in C_T (but not in C_t). Correspondingly, in variants I–III, the conventional value $C_T = 9$ per mil/°C is confirmed only as the least optimal value at maximal $C_t = 0.67 \pm 0.05$ ($C_tC_T = 6.0 \pm 0.5$ per mil/°C). Curve 3 in Figure 5a gives an example of corresponding temporal variations of the ice sheet surface temperature $\delta T_s(t)$ predicted by (8) at $C_tC_T = 6$ per mil/°C. Notice that

the influence of horizontal advection of ice, which is negligible for the calibration procedure due to the short distance between the drilling and the precipitation sites, may be significant for the older part of the temperature record [*Jouzel et al.*, 1996].

Thus this series of computations leads to an estimate of the deuterium-temperature slope close to its present-day spatial value (9 per mil/°C) and supports the standard practice of applying the latter to interpret Antarctic palaeodata [*Jouzel et al.*, 1987, 1993, 1996]. However, in spite of an agreement of the above estimates with experimental observations and theoretical predictions [e.g., *Lorius and Merlivat*, 1977; *Jouzel and Merlivat*, 1984; *Dahe et al.*, 1994], all the best fits demonstrate a significantly high magnitude of the target function $S \sim 0.11°$–$0.16°C$, i.e., about 20 times greater than that for the reconstructed harmonics in (3). This was additionally confirmed in computations for various b^0 and q_0. The result would not change either if a more detailed isotopic record was used in simulations.

Consequently, we suggest that there is a supplementary climatic signal in δT_s which does not exist in the scaled δD (or δT_i) record but is remembered in the borehole temperature. Accordingly, we modify (8) as

$$\delta T_s(t) = \frac{\delta D - 8\delta^{18}O_{sw}}{C_i C_T} - \frac{\alpha_{Ti} - \alpha_{Ts} C_i}{C_i} \cdot (K_i \delta\Delta - \alpha_L \delta^{18}O_{sw}) + \delta_p(t), \quad (9)$$

where $\delta_p(t)$ is a certain additional correction describing climatically induced difference between the thermal states of the ice sheet surface and the atmosphere (the top of the inversion layer) documented in the thermally transformed form in the glacier thickness.

The corresponding images of the δ_p signal in variants I–III can easily be distinguished in the experimental temperature-depth curve against the "background" temperature profiles simulated at $\delta_p \equiv 0$. They all are remarkably similar. The one calculated in variant III is plotted versus depth in Figure 4b. Its amplitude is about 0.4°C, which lies far beyond the estimated limits of the experimental errors.

As it has already been mentioned in the previous section, the comparison of the isotopic temperature record with the inferred surface temperature variations (see Figures 2b and 5a, curves 3 and 4) suggests that δ_p may primarily undergo precession oscillations. This supposition appears to be well grounded by taking into account that the last precession cycle is entirely documented in the borehole temperature profile (see Figure 1c). Thus at least additional precession signal δ_p (its recent period) is needed to correct the surface temperature variations δT_s in (9), while other components might be adjusted by an appropriate choice of a single parameter such as the product $C_i C_T$. Certainly, this is not the only approach that could be considered, and we actually do not have sufficient information in the borehole temperature memory to extend δ_p periodically back into the past. However, one of the reasons for a selective amplification of the precession climatic oscillations in the surface temperature, which makes the early Holocene temperatures on the ice sheet surface warmer and the LGM temperatures colder than it was thought before, could originate from the fact that the positive difference between the mean annual temperatures T_i and T_s is mainly a seasonal (winter) phenomenon. Hence as it was predicted for central Antarctica by *Short et al.* [1991], the precession signal in the seasonal temperature response (i.e., in the inversion strength)

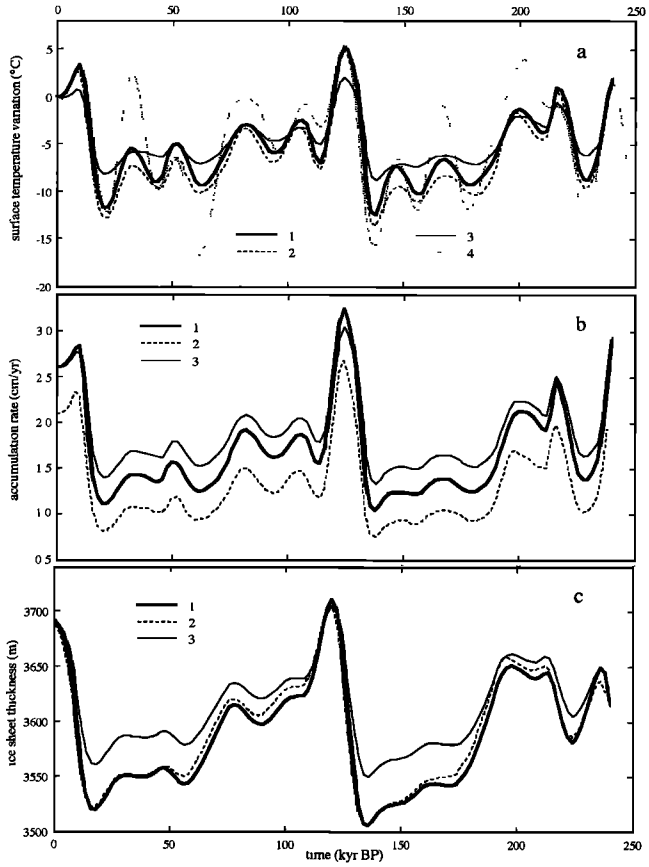

Figure 5. Reconstructed time series of palaeoenvironmental characteristics. (a) Various surface temperature-time curves reconstructed on the basis of the smoothed deuterium profile (Figure 2a). The coefficients in equations (5), (8), and (9) are adjusted at $C_i = 0.67$ to obtain the best correspondence between surface temperature variations and measured borehole temperature profile: (1) $C_i C_T = 4.5$ per mil/°C, $\alpha_p = 0.29$ (variant III in Figure 1a); (2) $C_i C_T = 3.9$ per mil/°C, $\alpha_p = 0.14$ (variant I); (3) $C_i C_T = 6$ per mil/°C, $\delta_p \equiv 0$ (variant III); (4) the inferred metronomic signal (variant III). Temperature variations are presented with respect to the reference point $T_s^0 = -57.9°C$. Curve 3 is consistent with standard practice to interpret the Vostok isotope profile [*Jouzel et al.*, 1987, 1993, 1996]. (b) Accumulation rate-time series deduced from the temperature variations at the top of the inversion layer. Curves 1–3 correspond to those in (a) at $C_i = 0.67$. (c) Past changes in the ice-sheet thickness at Vostok. Curves 1–3 are simulated using the accumulation rate-time curves displayed in Figure 5b with the same numbers.

to orbital forcing could have been essentially stronger than that in the mean annual temperature variations traced by δT_i.

Finally, since variations of the inversion and surface temperatures are assumed to be synchronous and orbitally driven, we can take the inferable components of δ_p proportional to the precession harmonics of the metronome given by (2):

$$\delta_p(t) = \alpha_p \sum_{i=3,4} [A_i \cos(\omega_i t) - B_i \sin(\omega_i t)], \quad (10)$$

$$-t_0 < t < 0.$$

The inverse problem of the palaeothermometer calibration is then formulated as a problem of the S-function minimization

with respect to C_T (i.e., the product $C_t C_T$) and α_p for different C_t in (5) and (9) at fixed A_i, B_i ($i = 3, 4$) in (10) taken as determined earlier in metronome (3).

The best-fit values of the product $C_t C_T$ turn out to be almost the same for different plausible conditions of the glacier dynamics, but they are noticeably (about 30%) less than in the starting computational experiments with (5) and (8). The extreme estimates are obtained in variants III and I, resulting in $C_t C_T = 4.8 \pm 0.3$ and 4.2 ± 0.3 per mil/°C, $\alpha_p = 0.29$ and 0.14, respectively, for $0.4 \leq C_t \leq 0.7$ with $S \sim 0.01°$–0.026°C. The reconstructed surface temperature variations are presented in Figure 5a by the solid and dashed lines (curves 1 and 2). Although the initial parameters (b^0 and σ) in these two cases differ considerably (see section 3), the corresponding surface temperatures appear to be very close, as well as their δ_p components. The difference in the best fit estimates of α_p just compensates the original deviation in the amplitudes of the precession metronomic harmonics in (10) in variants I and III. This result is very important and shows that (9) and (10) are almost uniquely constrained by the borehole temperature profile: all acceptable solutions of the inverse problem fall within the range between the two curves. It is not even, to a minor degree, influenced by the uncertainties in the timescale which is well established for the recent history. Obviously, relations (5), (9), and (10) are approximate, and containing only three parameters C_i, C_T, and α_p, they are less "flexible" than the sum of Milankovich harmonics in (3). For this reason the magnitude of the standard deviation S is somewhat higher than that reached in the metronomic reconstruction in section 3. Yet, it is now 10 times less than the level of discrepancy between the computed and the observed present-day temperature profiles with $\delta_p \equiv 0$ in (9).

The apparent uniqueness of the relationship between isotopic ratios δD and ice sheet surface temperature variations δT_s given by (9) still does not allow us to draw a definite conclusion about the value of C_T in (5) unless we fix the mean amplification coefficient (i.e., the factor C_t) relating long-term fluctuations (41-kyr and 100-kyr cycles) of δT_t to those of δT_s. The conventional estimate $C_T = 9$ per mil/°C, derived from geographical data [*Jouzel et al.*, 1993], can be confirmed as optimal for $C_t = 0.5 \pm 0.02$ in variants I–III. Alternative values of C_T lie within the range 5.8–6.5 per mil/°C, corresponding to the best fits in limiting cases I and III at $C_t = 0.67$. The factor $C_t \approx 0.5$ is closer to the observations by *Phillpot and Zillman* [1970] at Vostok. However, a greater magnitude of C_t [*Jouzel and Merlivat*, 1984; *Connolley*, 1996] and the reduced estimates of C_T seem to be more likely due to the close agreement (found in this case and discussed below) between GMTS and ice ages obtained by direct modeling of the ice sheet dynamics, as well as between present-day spatial variations of accumulation rate and those predicted by (2) and (5). These estimates cannot be considered as rigorous because the accumulation rate variations are not well known and parameter C_T also incorporates an additional uncertainty of the exponent factor η_b in (2).

6. Discussion and Other Glaciological Implications

One primary result of our study is that the introduction of an additional precession signal in the surface temperature variations noticeably improves the fit between the simulated and the measured borehole temperature profiles and leads to lower estimates of the temporal deuterium-temperature slope (5.8–6.5 per mil/°C). If our suggestion is correct, it implies that the glacial-interglacial temperature increase over central Antarctica was about 15°C in the ice sheet surface temperature and about 10°C in the inversion temperature. Besides, the annual temperature on the ice sheet surface and the inversion strength probably undergo relatively more intensive and selectively amplified oscillations in the precession band with an additional increase in their amplitudes of about 1.5°–2°C represented by the δ_p signal in (9) and (10). The mean Pleistocene-climate temperature on the glacier surface at Vostok is estimated as $\langle T_s \rangle = -64$°C and is about 6°C lower than its present-day value $T_s^0 = -57.9$°C. The surface temperature increased from −69.6°C in the LGM at 21 kyr B.P. to its Holocene maximum −54.6°C at 9 kyr B.P.

The reconstruction performed in this paper on the basis of the ice core isotope record (curves 1 and 2 in Figure 5a) appears to be much closer (especially for the recent 25-kyr interval) to metronomic temperature-time curve 4 than in previous interpretations (curve 3 in Figure 5a) based on the contemporary spatial isotope-temperature slope. Additional arguments for a higher estimate of the LGM-to-Holocene warming in Antarctica could be obtained from the analysis of crystal growth in the ice sheet [*Petit et al.*, 1987]. Recent interpretations of the GISP2 [*Cuffey et al.*, 1995] and GRIP [*Johnsen et al.*, 1995] ice core isotope records using borehole thermometry have revealed even greater changes (21°–22°C) in the surface temperature in Greenland. It should be noted that in both Greenland papers, δT_s is straightforwardly taken as a linear or parabolic function of $\delta^{18}O$ without distinction between inversion-layer, near-surface-air, and ice-sheet-surface temperatures. As against the unique situation in central Antarctica, accumulation rate in central Greenland is about 1 order of magnitude higher and the long-term climatic variations are not remembered separately in the temperature profile. For this reason the palaeothermometer calibration procedure might not have felt the selective amplification of the precession signal and a uniform relation between δT_s and $\delta^{18}O$ was quite acceptable. On the contrary, in the case of the Vostok isotope record, such a procedure (even a nonlinear one) would equally and enormously reduce not only the LGM temperature level but all glacial temperatures without a sufficient increase in Holocene temperatures. This, in accordance with the sensitivity tests performed in section 3, would lead to an unreasonable discrepancy between simulated and measured borehole temperature profiles in their deeper part.

Interestingly, we could easily relate now most of the events of the marine stages in benthic $\delta^{18}O$ (global ice volume) variations and their ages [*Martinson et al.*, 1987] to those of the corresponding climatic changes revealed in the surface temperature variations at Vostok (see Figures 1a, 5a, and Table 2). Such a procedure (not described in this paper) would result in the average lead of the polar temperature changes of about 2.9 ± 3.2 kyr. *Waelbroeck et al.* [1995] obtained almost the same phase difference of 3 ± 4 kyr for the two records in precession band. *Pichon et al.* [1992] deduced the phase lag estimate: 3–5 kyr between the benthic $\delta^{18}O$ signal and the southern SST fluctuations.

The new particularities in the isotope record interpretation lead to new predictions of the accumulation-rate and ice-sheet-surface-elevation variations in the past, which directly depend on δT_t in (2) and hence on the factor C_T in (5). Figures 5b and 5c illustrate the maximal possible fluctuations at $C_t = 0.67$

with the lower estimates of C_T. Curves 1 and 2 correspond to cases III and I at $C_T = 6.5$ and 5.8 per mil/°C, respectively, with the glacial-interglacial changes in the inversion temperature of about 10°C, while curves 3 are computed at conventional value $C_T = 9$ per mil/°C ($C_t C_T = 6$ per mil/°C, $C_t = 0.67$) for variant III. Obviously, the changes in the accumulation rate strongly depend on the estimate of the present-day precipitation b^0 but become relatively greater (compare curves 1 and 3 in Figure 5b) as C_T decreases. The amplitude of the ice thickness oscillations between glacial and interglacial stages might reach 200 m, i.e., about 50 m higher than it was simulated previously by *Salamatin and Ritz* [1996].

In all considered situations (variants I–III) the predicted ice melting rates w_0 at the ice sheet bottom are greater than zero and fall into the range $0.1 < w_0 < 0.3$ mm/yr.

Finally, we would like to return to the discussion of the deduced timescale (GMTS) and to its interpretation on the basis of the direct ice-flow modeling conducted by *Ritz* [1992] in order to compare and to match these two different (glaciological and "geophysical-metronome") approaches to ice core dating. An important result of Ritz's investigations is that plausible changes in spatial variation of accumulation rate along the ice-flow line upstream of Vostok to ridge B do not practically affect the thinning function which describes ice compression in the vertical direction. All predictions fall within the uncertainty range of ±0.025. Consequently, the ice age is straightforwardly determined by initial thickness of ice layers, i.e., by the accumulation rate at the time of their origin, at the location of their deposition.

Notice that the Holocene time interval 1.7–8.4 kyr B.P. in Table 2 yields exactly the mean present-day estimate of the accumulation rate at Vostok Station: $b^0 = 2.4$ cm/yr [*Barkov and Lipenkov*, 1996]. Furthermore, the direct qualitative examination (see Figure 3a) or quantitative analysis (see Table 2) of the timescale deduced from the borehole temperature profile allows us to distinguish three major segments on the age-depth curve with different slopes correlating to glacial and interglacial climatic stages. They are roughly given by the following time intervals: (1) 33–106, (2) 106–138, and (3) 138–200 kyr BP, which correspond to the depth ranges 630–1400, 1400–2000, and 2000–2500 m, respectively. According to *Ritz* [1992] the mean deposition distances of these layers are 70, 120, and 170 km upstream of Vostok, while their relative thinning is predicted to be 0.74, 0.59, and 0.38 ± 0.025, respectively. This, being applied to our timescale, immediately results in the following estimates of the mean accumulation rates (normalized by $b^0 = 2.4$ cm/yr), at which the three strata were formed: (1) 0.59 ± 0.016, (2) 1.32 ± 0.056, and (3) 0.88 ± 0.058. At the same time, the relative accumulation rate $\bar{b}$ at Vostok simulated in variants I and III (see Figure 5b) are practically identical and for each of the three climatic time intervals its mean values at $C_t = 0.67$ are (1) 0.6, (2) 0.78, and (3) 0.54.

Thus we come to the following conclusion: the estimate of the mean accumulation rate, $\bar{b} \approx 0.6$, in the 100-km vicinity of Vostok Station during the glacial 30- to 100-kyr period derived from GMTS on the basis of the ice-flow modeling coincides with that directly calculated from (2) and (5) at the best-fit (30% reduced) isotope-temperature ratio $C_T = 5.8$–6.5 per mil/°C. As was shown by *Ritz* [1992], such a reduction was also necessary to adjust the latter predictions to the relative precipitation given by the ice core cosmic ^{10}Be record [*Raisbeck et al.*, 1987] within the same depth interval 630–1400 m. This actually brings together different approaches to the ice age dating as well as the different estimates of accumulation rate variations in the past.

The next step is to compare the deduced accumulation rates at the locations which are closer to ridge B (i.e., approximately 120 and 170 km from Vostok Station) to those simulated for Vostok with $C_t = 0.67$ at the same times of ice deposition. The corresponding values of their ratios are 1.69 ± 0.07 and 1.63 ± 0.11 for the intervals 106–138 and 138–200 kyr BP, respectively. This is in striking agreement with the enhancement factor 1.65 in spatial distribution of the net accumulation which was derived by *Jouzel et al.* [1993] from the independent comparison of the ice core isotopic records at Vostok Station and at dome B. This result gives us another piece of evidence that both chronologies deduced from the borehole thermometry and on the basis of the direct ice flow modeling are identical and realistic if we assume the accumulation rate in the vicinity of ridge B (beginning from 100 km upstream along the Vostok flow line) uniform and 1.5–1.75 times higher (at least during the period 106–200 kyr BP) than its current magnitude at Vostok Station, provided that the isotope-inversion temperature ratio C_T in (5) is about 6 per mil/°C (i.e., $C_t \approx 0.67$, $C_t C_T \approx 4$ per mil/°C). *Ritz* [1992] arrived at a similar conclusion by fitting hydrodynamically simulated ice ages to dust age markers [*Petit et al.*, 1990]. It was also shown in this study that the factor η_b in (2) could be influenced by different precipitation mechanisms within 6–11%. This would also affect the preferable choice of the C_T value. Summarizing the above discussions, we come to the following estimates of the calibration parameters in (5) and (9): $C_t C_T \approx 4.5 \pm 0.5$ per mil/°C with $C_t = 0.6 \pm 0.1$ and $C_T = 7.5 \pm 1.5$ per mil/°C, including all possible limiting situations. The main uncertainty here arises from the factor C_t.

7. Conclusion

The temperature profile measured in the deep borehole at Vostok Station provides an important additional constraint for ice core dating and isotopic palaeothermometer calibration. The major achievements of the study are thought to be (1) Geophysical-Metronome Timescale (GMTS) which estimates age-depth relation for the Vostok ice core with a standard error of ±3.0–4.5 kyr and predicts the ice core age of 241 kyr at a depth of 2760 m, and (2) the inferred smoothed timeseries of surface temperature variations matched to both the stacked ice core deuterium record and the present-day borehole temperature profile.

Assuming that surface temperatures could undergo more intensive precession oscillations than those of inversion temperatures, we revealed 30% stronger temperature changes (surface temperature increased by 15°C during the last deglacial transition) than it was predicted from contemporary spatial isotope-temperature correlation in Antarctica. The new interpretation of the Vostok isotope record would be in qualitative agreement with the findings by *Cuffey et al.* [1995] and *Johnsen et al.* [1995] for the GRIP and GISP2 cores, with however a significantly smaller difference between the estimates based on water isotopes and borehole palaeothermometry for Antarctica than for Greenland.

A joint employment of our dating procedure and other approaches [*Ritz*, 1992; *Jouzel et al.*, 1996; *Waelbroeck et al.*, 1995] could provide the Vostok ice core timescale supported by ice-flow modeling, borehole geophysical data, as well as direct orbital tuning, and consistent with the SPECAMP chronology

over at least 400 kyr [*Petit et al.*, 1997]. The results of our study additionally stress a necessity of multilateral approach to interpretation of the ice core isotope records.

Acknowledgments. This collaborative study was supported by the European Science Foundation and also by the Ministry for General and Professional Education and by the State Committee for Science and Technologies of the Russian Federation. The authors thank Yu. Rydvan and A. Volkov for providing the borehole-thermometry data. Our special gratitude should be expressed to C. Lorius, C. Waelbroeck, C. Ritz, and T. Hondoh for useful discussions and important comments. The work has gained much from the comments of the reviewers of this paper.

References

Aver'yanov, V. G., Gradienty temperatury vozdukha u poverkhnosty lednikovogo pokrova Antarktidy (Air temperature gradients at the Antarctic ice sheet surface), in *Geograficheskiye i Glyatsiologicheskaye Issledovaniya v Polyarnikh Stranakh*, Gidrometeoizdat, pp. 55–60, St. Petersburg, Russia, 1988.

Barkov, N. I., and V. Y. Lipenkov, Nakopleniye snega v rayone stantsii Vostok, Antarktida, v 1970–1992 gg. (Snow accumulation at Vostok Station, Antarctica, 1970–1992], *Mater. Glyatsiol. Issled.*, *80*, 87–88, 1996.

Barkov, N. I., K. V. Blinov, V. N. Petrov, and A. N. Salamatin, Chislennyye eksperimenty po rekonstruktsii paleoklimata na osnove rezul'tatov termometrii glubokoy skvazhiny na stantsii Vostok v Antarktide (Numerical experiments on paleoclimate reconstruction from temperature measurements in the deep borehole drilled in the ice sheet at Vostok Station, Antarctica), *Mater. Glyatsiol. Issled.*, *67*, 116–121, 1989.

Barnola, J. M., D. Raynaud, Y. S. Korotkevich, and C. Lorius, Vostok ice core provides 160,000-year record of atmospheric CO_2, *Nature*, *329*(6138), 408–414, 1987.

Barnola, J. M., P. Pimienta, D. Raynaud, and Y. S. Korotkevich, CO_2-climate relationship as deduced from the Vostok ice core: A re-examination based on new measurements and on a revaluation of the air dating, *Tellus*, *43*(B), 83–90, 1991.

Berger, A. L., Long-term variations of daily insolation and Quaternary climatic changes, *J. Atmos. Sci.*, *35*, 2362–2367, 1978.

Budd, W. F., and N. W. Young, Application of modelling techniques to measured profiles of temperatures and isotopes, in *The Climatic Record in Polar Ice Sheets*, edited by G. de Q. Robin, pp. 150–177, Cambridge University Press, New York, 1983.

Chappellaz, J., J. M. Barnola, D. Raynaud, Y. S. Korotkevich, and C. Lorius, Ice core record of atmospheric methane over the past 160,000 years, *Nature*, *345*(6271), 127–131, 1990.

Clemens, S. C., and W. L. Prell, Late Pleistocene variability of Arabian Sea summer monsoon winds and continental aridity: Eilin records from the lithogenic component of deep-sea sediments, *Paleoceanography*, *5*(2), 109–145, 1990.

Connolley, W. M., The Antarctic temperature inversion, *Int. J. Climatol.*, *16*, 1333–1342, 1996.

Cuffey, K. M., R. B. Alley, P. M. Grootes, J. M. Bolzan, and S. Anandakrishnan, Calibration of the $\delta^{18}O$ isotopic paleothermometer for central Greenland, using bore hole temperatures, *J. Glaciol.*, *40*(135), 341–349, 1994.

Cuffey, K. M., G. D. Clow, R. B. Alley, M. Stuiver, E. D. Waddington, and R. W. Saltus, Large Arctic temperature change at the Glacial-Holocene transition, *Science*, *270*, 455–458, 1995.

Dahe, Q., J. R. Petit, J. Jouzel, and M. Stievenard, Distribution of stable isotopes in surface snow along the route of the 1990 International Trans-Antarctica Expedition, *J. Glaciol.*, *40*(134), 107–118, 1994.

Dahl-Jensen, D., and S. J. Johnsen, Palaeotemperatures still exist in the Greenland ice sheet, *Nature*, *320*(6059), 250–252, 1986.

Dansgaard, W., Stable isotopes in precipitation, *Tellus*, *16*, 436–468, 1964.

Dansgaard, W., S. J. Johnsen, H. B. Clausen, C. U. Hammer, and N. Grundestrup, Stable isotope glaciology, *Medd. Groenl.*, *197*(2), 1–53, 1973.

Dansgaard, W., et al., Evidence for general instability of past climate from a 250-kyr ice-core record, *Nature*, *364*(6434), 218–220, 1993.

Drewry, D. J. (Ed)., *Antarctica: Glaciological and geophysical folio*, Scott Polar Res. Inst., Cambridge, Mass., 1983.

Genthon, C., J. M. Barnola, D. Raynaud, C. Lorius, J. Jouzel, N. I. Barkov, Y. S. Korotkevich, and V. M. Kotlyakov, Vostok ice-core: Climatic response to CO_2 and orbital forcing changes over the last climatic cycle, *Nature*, *329*(6138), 414–418, 1987.

Imbrie, J., et al., On the structure and origin of major glaciation cycles, 1, Linear responses to Milankovitch forcing, *Paleoceanography*, *7*(6), 701–738, 1992.

Imbrie, J., et al., On the structure and origin of major glaciation cycles, 2, The 100,000-year cycle, *Paleoceanography*, *8*(6), 699–735, 1993.

Johnsen, S., W. Dansgaard, and J. W. C. White, The origin of Arctic precipitation under present and glacial conditions, *Tellus*, *41B*, 452–468, 1989.

Johnsen, S., D. Dahl-Jensen, W. Dansgaard, and N. Grundestrup, Greenland palaeotemperatures derived from GRIP borehole temperature and ice-core isotope profiles, *Tellus*, *47B*(5), 624–629, 1995.

Jouzel, J., and L. Merlivat, Deuterium and oxygen 18 in precipitation: Modeling of the isotopic effects during snow formation, *J. Geophys. Res.*, *89*, 11,749–11,757, 1984.

Jouzel, J., C. Lorius, J. R. Petit, C. Genthon, N. I. Barkov, V. M. Kotlyakov, and Y. S. Korotkevich, Vostok ice-core: A continuous isotope temperature record over the last climatic cycle (160,000 years), *Nature*, *329*(6138), 403–408, 1987.

Jouzel, J., et al., Extending the Vostok ice-core record of palaeoclimate to the penultimate glacial period, *Nature*, *364*(6436), 407–412, 1993.

Jouzel, J., R. D. Koster, R. J. Suozzo, and G. L. Russell, Stable water isotope behavior during the last glacial maximum: A GCM analysis, *J. Geophys. Res.*, *99*, 25,791–25,801, 1994.

Jouzel, J., et al., Climatic interpretation of the recently extended Vostok ice records, *Clim. Dyn.*, *12*, 513–521, 1996.

Kapitsa, A. P., J. K. Ridley, G. de Q. Robin, M. J. Siegert, and I. A. Zotikov, A large deep freshwater lake beneath the ice of central East Antarctica, *Nature*, *381*(6584), 684–686, 1996.

Le Meur, E., and P. Huybrechts, A comparison of different ways of dealing with isostasy: Examples from modeling the Antarctic ice sheet during the last glacial cycle, *Ann. Glaciol.*, *23*, 309–317, 1996.

Lliboutry, L., A critical review of analytical approximate solutions for steady state velocities and temperatures in cold ice-sheets, *Z. Gletscherkd. Glazialgeol.*, *15*(2), 135–148, 1979.

Lorius, C., and L. Merlivat, Distribution of mean surface stable isotope values in East Antarctica: Observed changes with depth in the coastal area, *Int. Assoc. Hydrol. Sci. Publ. 118*, *1975*, 127–137, 1977.

Lorius, C., J. Jouzel, C. Ritz, L. Merlivat, N. I. Barkov, Y. S. Korotkevich, and V. M. Kotlyakov, A 150,000 year climatic record from Antarctic ice, *Nature*, *316*(6029), 591–596, 1985.

Martinson, D. G., N. G. Pisias, J. D. Hays, J. Imbrie, T. C. Moore, and N. J. Shackleton, Age dating and the orbital theory of ice ages: Development of a high-resolution 0 to 300,0000-year chronostratigraphy, *Quat. Res.*, *27*(1), 1–29, 1987.

Palaeogeography, Palaeoclimatology, Palaeoecology, Climatic change inferred from underground temperatures (special issue), *Palaeogeogr., Palaeoclimatol., Palaeoecol.*, *98*(2/4), 1992.

Petit, J. R., P. Duval, and C. Lorius, Long-term climatic changes indicated by crystal growth in polar ice, *Nature*, *326*(6108), 62–64, 1987.

Petit, J. R., L. Mounier, J. Jouzel, Y. S. Korotkevich, V. M. Kotlyakov, and C. Lorius, Paleoclimatological and chronological implications of the Vostok core dust record, *Nature*, *343*(6253), 56–58, 1990.

Petit, J. R., et al., Four climatic cycles depicted in the Vostok ice (Antarctica), *Nature*, *387*, 359–360, 1997.

Phillpot, H. R., and J. W. Zillman, The surface temperature inversion over the Antarctic continent, *J. Geophys. Res.*, *75*(21), 4161–4169, 1970.

Pichon, J.-J., L. D. Labeyrie, G. Bareille, M. Labracherie, J. Duprat, and J. Jouzel, Surface water temperature changes in the high latitudes of the southern hemisphere over the last glacial-interglacial cycle, *Paleoceanography*, *7*, 289–318, 1992.

Raisbeck, G. M., F. Yiou, D. Bourles, C. Lorius, J. Jouzel, and N. I. Barkov, Evidence for two intervals of enhanced ^{10}Be deposition in Antarctic ice during the last glacial period, *Nature*, *326*(6110), 62–64, 1987.

Ridley, J. K., W. Cudlip, and S. W. Laxon, Identification of subglacial

lakes using ERS-1 radar altimeter, *J. Glaciol.*, *39*(133), 625–634, 1993.

Ritz, C., Interpretation of the temperature profile measured at Vostok, East Antarctica, *Ann. Glaciol.*, *12*, 138–144, 1989.

Ritz, C., Un modèle thermo-mecanique d'évolution pour le bassin glaciaire Antarctique Vostok-glacier Byrd: Sensibilité aux valeurs des paramèters mal connus, Ph.D. thesis, d'Etat Univ. Joseph Fourier, Grenoble, France, 1992.

Robin, G. de Q., Reconciliation of temperature-depth profiles in polar ice sheets with surface temperatures deduced from oxygen-isotope profiles, *J. Glaciol.*, *16*(74), 9–22, 1976.

Robin, G. de Q., Ice cores and climatic change, *Phil. Trans. R. Soc. London*, *280*(B), 143–168, 1977.

Salamatin, A. N., Ice sheet modeling taking account of glacier ice compressibility, *Int. Assoc. Hydrol. Sci. Publ. 208, 1990*, 183–192, 1991.

Salamatin, A. N., and C. Ritz, A simplified multi-scale model for predicting climatic variations of the ice sheet surface elevation in the Central Antarctica, *Ann. Glaciol.*, *23*, 28–35, 1996.

Salamatin, A. N., V. Y. Lipenkov, and K. V. Blinov, Vostok (Antarctica) climate record timescale deduced from the analysis of a borehole-temperature profile, *Ann. Glaciol.*, *20*, 207–214, 1994.

Salamatin, A. N., V. Y. Lipenkov, and K. V. Blinov, Vosstanovleniye klimatischeskikh izmeneniy temperatury na poverkhnosti antarkticheskogo lednikovogo pokrova v proshlom po resul'tatam temperaturnikh izmereniy v glubokikh skvazhinakh na stantsii Vostok, (Reconstruction of temperature climatic variations on the Antarctic ice sheet in the past from temperature measurements in deep boreholes at Vostok Station), *Mater. Glyatsiol. Issled.*, *79*, 75–82, 1995.

Shackleton, N., J. Le, A. Mix, and M. A. Hall, Carbon isotope records from Pacific surface waters and atmospheric carbon dioxide, *Quat. Sci. Rev.*, *11*, 387–400, 1992.

Short, D. A., J. G. Mengel, T. J. Crowley, W. T. Hyde, and G. R. North, Filtering of Milankovitch cycles by Earth's geography, *Quat. Res.*, *35*, 157–173, 1991.

Siegert, M. J., and J. A. Dowdeswell, Spatial variations in heat at the base of the Antarctic ice sheet from analysis of the thermal regime above subglacial lakes, *J. Glaciol.*, *42*(142), 501–509, 1996.

Sowers, T., M. Bender, D. Raynaud, and Y. S. Korotkevich, The $\delta^{15}N$ of N_2 in air trapped in polar ice: A tracer of gas transport in the firn and a possible constraint on ice age-gas age difference, *J. Geophys. Res.*, *97*, 15,683–15,697, 1992.

Sowers, T., M. Bender, L. Laberyrie, D. Martinson, J. Jouzel, D. Raynaud, J. J. Pichon, and Y. S. Korotkevich, A 135,000-year Vostok-SPECMAP common temporal framework, *Paleoceanography*, *8*(6), 737–766, 1993.

Vostretsov, R. N., D. N. Dmitriyev, O. F. Putikov, K. V. Blinov, and S. V. Mitin, Osnovnyye rezul'taty geofizicheskikh issledovaniy glubokikh skvazhin i ledyanogo kerna v Vostochnoy Antarktide (Main results of geophysical studies of deep boreholes and the ice core in East Antarctica), *Mater. Glyatsiol. Issled.*, *51*, 172–178, 1984.

Waelbroeck, C., J. Jouzel, L. Labeyrie, C. Lorius, M. Labracherie, M. Stievenard, and N. I. Barkov, Comparing the Vostok ice deuterium record and series from Southern Ocean core MD 88-770 over the last two glacial-interglacial cycles, *Clim. Dyn.*, *12*, 113–123, 1995.

A. N. Salamatin, Department of Applied Mathematics, Kazan State University, 18, Kremlyevskaya Street, Kazan 420008, Russia.

N. I. Barkov and V. Y. Lipenkov, Arctic and Antarctic Research Institute, 38, Bering Street, St. Petersburg 199397, Russia.

J. Jouzel, Laboratoire de Modélisation du Climat et de l'Environnement, CEA/DSM CE Saclay, 91191, Gif/Yvette, France.

J. R. Petit and D. Raynaud, Laboratoire de Glaciologie et Géophysique de l'Environnement, 54, Rue Molière, Domaine Universitaire, B.P. 96, 38402, St.-Martin-d'Hères Cedex, France.

(Received March 8, 1996; revised May 14, 1997;
accepted August 7, 1997.)